

# Diffusion and stability in perturbed non convex integrable systems

**Massimiliano Guzzo**

Dipartimento di Matematica Pura ed Applicata Università degli Studi di Padova, via  
Belzoni 7, 35131 Padova, Italy

**Elena Lega**

Observatoire de Nice, Bv. de l'Observatoire, B.P. 4229, 06304 Nice cedex 4, France.

**Claude Froeschlé**

Observatoire de Nice, Bv. de l'Observatoire, B.P. 4229, 06304 Nice cedex 4, France.

**Abstract.** The Nekhoroshev theorem has become an important tool for explaining the long-term stability of many quasi-integrable systems of interest in physics. The action variables of systems that satisfy the hypotheses of Nekhoroshev theorem remain close to their initial value up to very long times, that grow exponentially as an inverse power of the perturbation's norm. In this paper we study some of the simplest systems that do not satisfy the hypotheses of Nekhoroshev theorem. These systems can be represented by a perturbed Hamiltonian whose integrable part is a quadratic non-convex function of the action variables. We study numerically the possibility of action diffusion over short times for these systems (continuous or maps) and we compare it with the so-called Arnold diffusion. More precisely we find that, except for very special non-convex functions, for which the effect of non convexity concerns low order resonances, the diffusion coefficient decreases faster than a power law (and possibly exponentially) of the perturbation's norm. According to the theory, we find that the diffusion coefficient as a function of the perturbation's norm decreases slower than in the convex case.

## 1. Introduction

Many physical systems can be represented adding a perturbation to integrable systems whose motions are completely known, and specifically are quasi-periodic. The celebrated KAM ([1], [2], [3], [4]) and Nekhoroshev theorems ([5]) are the milestones in the understanding of the long-term stability of quasi-integrable systems. In particular, in recent years, the Nekhoroshev theorem has been largely used to investigate the long-term stability of dynamical systems ([6], [7], [8], [9], [10], [11]). In the Hamiltonian case, this theorem can be stated as follows. Let us consider hamiltonians of the form:

$$H(I, \varphi) = h(I) + \varepsilon f(I, \varphi) \quad , \quad (1)$$

where  $I \in \mathcal{D}$  ( $\mathcal{D} \subseteq \mathbb{R}^n$  open),  $\varphi \in \mathbb{T}^n$ ,  $h$  and  $f$  are analytic and  $h$  satisfies a suitable geometric condition called 'steepness'. Then, there exist positive constants  $a, b, c, d, \varepsilon_0$  such that for any  $|\varepsilon| < \varepsilon_0$  the actions remain near their initial value:

$$|I(t) - I(0)| \leq c\varepsilon^a \quad (2)$$

up to the exponentially long-times:

$$|t| \leq d \exp\left(\frac{\varepsilon_0}{\varepsilon}\right)^b . \quad (3)$$

The values of the constants  $a$  and  $b$  depend on the steepness properties of  $h$  ([5], [12], [13]). The constant  $b$  is particularly important to characterize stability times.

The simplest example of steep functions is provided by convex functions, i.e. by functions  $h$  such that at any point  $I \in \mathcal{D}$  satisfy:

$$\left(\frac{\partial^2 h}{\partial I^2}(I)u \cdot u = 0 \quad , \quad u \in \mathbb{R}^n\right) \Rightarrow u = 0 \quad ,$$

and by quasi-convex functions, which satisfy the weaker condition:

$$\left(\frac{\partial^2 h}{\partial I^2}(I)u \cdot u = 0 \quad , \quad \nabla h(I) \cdot u = 0 \quad , \quad u \in \mathbb{R}^n\right) \Rightarrow u = 0 \quad .$$

In the convex and quasi-convex case the value of the constant  $b$  is the bigger one among all steep cases. Precisely, it is ([14], [15]):

$$b = \frac{1}{2n} . \quad (4)$$

An exponential stability result have been proved also for quasi-integrable symplectic maps ([16], [17], [18]), precisely for maps which can be written in the implicit form:

$$\varphi_j = \varphi'_j + \frac{\partial h}{\partial I_j}(I) + \varepsilon \frac{\partial f}{\partial I_j}(\varphi', I) \quad , \quad I'_j = I_j + \varepsilon \frac{\partial f}{\partial \varphi_j}(\varphi', I) \quad , \quad j = 1, \dots, n \quad (5)$$

with  $f$  analytic and  $h$  convex. Kuksin, Pöschel and Guzzo treat the convex case, but their results extend also to the larger class of the so-called P-steep functions (whose definition is given by Nekhoroshev in his 1977 article; quasi-convex functions are not P-steep).

However, most interesting systems (for example, the system describing the motion of an asteroid in the Main Belt of our solar system, see [6], [7]) do not satisfy the hypotheses of the Nekhoroshev theorem, in its standard formulation, because they are represented by a non steep hamiltonian  $h$ . For example, this happens when  $h$  is properly degenerate (such as the hamiltonian of the Kepler problem and of the Euler-Poinsot rigid body), i.e. it does not depend on some action variables. For many of these systems the degeneracy can be, in some sense, removed by perturbation techniques adapted to the system ([3], [6], [19], [20]). However there are non steep functions even among the non-degenerate functions  $h$ . We find the quadratic non-convex functions among the simplest non-degenerate functions which are not steep (nor P-steep) in some points. This paper is dedicated to the numerical investigation of the real possibility of diffusion of the actions in times much smaller than (3) for these quasi-integrable systems.

The paper is organized as follows. In section 2 we will give the mathematical framework and explain the mechanism for fast diffusion. Section 3 provides the model problem used for our numerical experiments. In section 4 we recall the method for detecting the geography of resonances and we show examples of diffusion along resonances in the non convex case. A measure of the variation of the diffusion coefficient as a function of the perturbing parameter is provided in section 5. We discuss in Section 6 the diffusion properties for different values of  $\alpha$ . The conclusion is provided in section 7. A review of the Fast Lyapunov Indicator method is given in the Appendix.

## 2. Mathematical framework

In this section we list the fundamental hypotheses and terminology that we will use through the paper.

i) *We strictly refer to quasi-integrable systems*, i.e. to Hamiltonian systems with Hamilton functions of the form (1) or to symplectic maps of the form (5).

ii) *The functions  $h, f$  are such that the Hamiltonian system (1) and the map (5) satisfy the hypotheses of KAM theorem (for quasi-integrable maps see [16],[17],[18]) for suitably small  $\varepsilon$ .* It is sufficient that  $h$  and  $f$  are analytic and  $h$  is non-degenerate or (only for Hamiltonian systems) isoenergetically non-degenerate.

iii) *We consider values of the perturbing parameter  $\varepsilon$  so small that KAM theorem applies.* This implies that the phase space is filled with a set  $\mathcal{K}$  of large measure made of invariant tori. Any motion with initial condition on  $\mathcal{K}$  is perpetually stable, so that instability can occur only on the complementary set of  $\mathcal{K}$ , which we call the *Arnold web*. The projection of the Arnold web on the action space  $\mathcal{D}$  lies on a neighbourhood of the manifolds:  $k \cdot \nabla h(I) = 0$ , with  $k \in \mathbb{Z}^n \setminus 0$ . Its complement is open and dense. With an abuse of terminology, we will use the term 'resonance' to indicate the manifold  $k \cdot \nabla h(I) = 0$ , as well as its neighbourhood which is in the Arnold web.

iv) We say that a motion  $(I(t), \varphi(t))$  is 'unstable' if there exists a time  $t$  such that the actions explore macroscopic regions of a given action domain  $B$ :

$$\|I(t) - I(0)\| \geq \frac{\text{diam}B}{2} . \quad (6)$$

Moreover, we say that the  $N$  motions  $(I^{(j)}(t), \varphi^{(j)}(t))$ ,  $j = 1, \dots, N$ , diffuse in the action space if the average evolution of the squared distance of the actions from their initial value grows linearly with time; i.e. there exists a constant  $D > 0$  such that:

$$\frac{\sum_{j=1}^N (I^{(j)}(t) - I^{(j)}(0))^2}{N} \sim D t \quad (7)$$

for all  $t$ .

v) If the system satisfies (i), (ii), (iii) and moreover  $h$  is steep (P-steep for maps) then also the Nekhoroshev theorem applies and any eventual instability of the actions occurs

only on times that grow exponentially with a positive power of  $1/\varepsilon$ . Any motion diffusion for a system satisfying (i), (ii), (iii) and the steepness hypothesis will be called Arnold diffusion. Though Arnold diffusion occurs on these very long times, the techniques that we introduced in [23],[25] allow its numerical detection. The first detection of global Arnold diffusion in quasi-integrable systems has been described in [26].

vi) This paper concerns the real possibility of diffusion for systems that satisfy (i), (ii) and (iii), but whose  $h$  is not steep (P-step for maps), so that in principle instability is possible already on times of order  $1/\varepsilon$ .

We first review the mechanism producing instability for quasi-integrable systems with non-convex quadratic functions  $h(I)$ , for both hamiltonian systems and maps. We will then investigate numerically the real possibility of diffusion using quasi-integrable maps, for which numerical experiments are simpler than the hamiltonian case.

Nekhoroshev, in his 1977 article, provided as an example of fast diffusion in non convex (and non steep) systems, the hamiltonian:

$$H = \frac{I_1^2}{2} - \frac{I_2^2}{2} - \varepsilon \sin(\varphi_1 + \varphi_2) \quad , \quad (8)$$

that has some special solutions with the actions moving at a speed of order  $\varepsilon$ :

$$\begin{aligned} I_1(t) &= \varepsilon t & , & & I_2(t) &= \varepsilon t \\ \varphi_1(t) &= \frac{1}{2}\varepsilon t^2 & , & & \varphi_2(t) &= -\frac{1}{2}\varepsilon t^2 \quad . \end{aligned} \quad (9)$$

To illustrate the mechanism producing this fast diffusion, it is instructive to consider a generic perturbation of the non-convex function  $h = \frac{I_1^2}{2} - \frac{I_2^2}{2}$ , such as:

$$H = \frac{I_1^2}{2} - \frac{I_2^2}{2} + \varepsilon f(\varphi_1, \varphi_2) \quad .$$

This system is quasi-integrable with non-degenerate integrable approximation  $h$ , and therefore the KAM theorem applies to it. However,  $h$  is not isoenergetically non-degenerate on the lines  $I_1 = \pm I_2$ , and therefore action diffusion can occur only near these lines (the systems has  $n = 2$ ), that we call escape lines.

The escape lines correspond also to the resonances:  $\dot{\varphi}_1 \pm \dot{\varphi}_2 = 0$ , and therefore, near the line  $I_1 = I_2$  (for simplicity we choose one escape line), by usual normal form construction the hamiltonian is conjugate by means of a near-to-identity canonical transformation to the resonant normal form:

$$\tilde{H} = H_0 + \varepsilon \exp - \left( \frac{\varepsilon_0}{\varepsilon} \right)^b r(I, \varphi)$$

with  $H_0$  of the form:

$$H_0 = \frac{I_1^2}{2} - \frac{I_2^2}{2} + \varepsilon u(I, \varphi_1 + \varphi_2) \quad .$$

The dynamics of the normal form  $H_0$  is such that the actions can move only on the line parallel to the vector:  $(1, 1)$ , which is also parallel to the resonance related to the

harmonic  $\varphi_1 + \varphi_2$ . Therefore, with suitable perturbations (for example such that  $H_0$  has the form (8)), actions with initial conditions in the resonance  $I_1 = I_2$  can move indefinitely at a speed of order  $\varepsilon$  without leaving the resonance.

Such a diffusion mechanism is not possible in the convex case:

$$H = \frac{I_1^2}{2} + \frac{I_2^2}{2} - \varepsilon \sin(\varphi_1 + \varphi_2) \quad .$$

In fact, the hamiltonian is isoenergetically non degenerate and KAM theorem prevents the diffusion of the actions (if  $n > 2$  diffusion can exist, but only on exponentially long times). Analyzing more closely the dynamics, the resonant normal form for a generic resonance:  $k_1\dot{\varphi}_1 + k_2\dot{\varphi}_2$  is defined near the line of the action plane:

$$k_1 I_1 + k_2 I_2 = 0 \quad , \quad (10)$$

and has the form:

$$\tilde{H} = H_0 + \varepsilon \exp - \left( \frac{\varepsilon_0}{\varepsilon} \right)^b r(I, \varphi)$$

with:

$$H_0 = \frac{I_1^2}{2} + \frac{I_2^2}{2} + \varepsilon u(I, k_1\varphi_1 + k_2\varphi_2) \quad .$$

The dynamics of  $H_0$  can move the actions only on the line parallel to the vector:  $(k_1, k_2)$ , usually called line of fast drift, which is perpendicular to the resonant line (10). Therefore, there cannot be a diffusion along the resonance with speed of order  $1/\varepsilon$ , and only the exponentially small remainder can force an exponentially slow diffusion along it (if  $n > 2$ ).

This is the mechanism underlying the exponential stability predicted by the Nekhoroshev theorem, and it is explained in several papers ([5], [21], [7]).

We now consider more generic quadratic integrable hamiltonians with 2 degrees of freedom, i.e. functions  $h$  of the form:

$$h = \frac{1}{2} AI \cdot I \quad , \quad (11)$$

where  $A$  is a 2-dimensional symmetric square matrix. The previous argument should provide that a condition which is sufficient to prevent the fast diffusion along a given resonance (as in the example by Nekhoroshev) is that the line of fast drift is not contained in the resonance. To be definite, for any  $k \in \mathbb{Z}^2 \setminus 0$ , the resonance  $k \cdot \dot{\varphi} = 0$  is defined by the equation:

$$k \cdot AI = 0 \quad ,$$

while the line of fast drift, in the action plane, is parallel to the vector  $k$ . Therefore, a fast diffusion should be possible only if this line is contained in the resonance, which happens only if  $Ak \cdot k = 0$ . In the rest of the paper we will call 'fast diffusion' any diffusion of orbits occurring for systems satisfying ((i), (ii) and (iii)) taking place on resonances of the Arnold web characterized by the fact that a space of fast drift is contained in the resonance.

Fast diffusion in the resonance  $k \cdot AI = 0$  is prevented if  $k$  satisfies $\ddagger$ :

$$Ak \cdot k \neq 0 \quad .$$

Convex hamiltonians satisfy this condition for any vector  $u \in \mathbb{R}^2 \setminus 0$ , and therefore also for any integer vector  $k \in \mathbb{Z}^2 \setminus 0$ .

Morbidelli and Guzzo ([7], see caption of figure 10) remarked that, also in the non-convex quadratic case, fast diffusion can be prevented: for example, for the following non-convex hamiltonian:

$$H = \frac{I_1^2}{2} - I_2^2 \quad ,$$

the equation:

$$u \cdot Au = 0 \quad \iff \quad u_1^2 - 2u_2^2 = 0$$

has the only non trivial solutions  $u_1 = \pm\sqrt{2} u_2$  and therefore the direction  $(u_1, u_2) = u_2(\sqrt{2}, 1)$  cannot be a direction of fast drift (which necessary requires  $u_1/u_2 \in \mathbb{Q}$ ).

Following the idea of Morbidelli and Guzzo, all the quadratic hamiltonians:  $h = \frac{1}{2}AI \cdot I$  with  $A$  non-convex, but satisfying:

$$(Ak \cdot k = 0 \quad \text{and} \quad k \in \mathbb{Z}^2) \quad \implies \quad k = 0 \quad (12)$$

are not compatible with fast diffusion $\S$ . For example, the function:

$$h = \frac{1}{2}(I_1^2 - \alpha I_2^2) \quad , \quad (13)$$

with  $\alpha > 0$ , is non-convex (nor step), but is compatible with fast diffusion only if  $\sqrt{\alpha} \in \mathbb{Q}$ , i.e. for  $\alpha$  of the form:

$$\alpha = \frac{n_1^2}{n_2^2} \quad (14)$$

with  $n_1, n_2 \in \mathbb{N}$ .

We will call 'rationally convex' a function  $h(I_1, I_2)$  such that its hessian matrix satisfies condition (12) at any point of its domain. Function (13) is not convex if  $\alpha \geq 0$ , but is rationally convex if  $\sqrt{\alpha} \in \mathbb{R}/\mathbb{Q}$ ,

For  $n > 2$  the condition of rational convexity slightly complicates, because the possibility of multiple resonance conditions forces us to take into consideration fast drift planes of dimension ranging from 1 to  $n - 1$ . Precisely, we give the following:

**Definition.** We say that the  $n$ -dimensional square matrix  $A$  is rationally convex if for any set of independent integer vectors  $k^1, \dots, k^d \in \mathbb{Z}^n$ , with  $d \in \{1, \dots, n - 1\}$ , denoting with  $\tilde{K}$  the  $d \times n$  matrix whose columns are the vectors  $k^i$ , it is:

$$\det(\tilde{K}^T A \tilde{K}) \neq 0 \quad . \quad (15)$$

$\ddagger$  More precisely in order to prove exponential stability one should require some algebraic condition such as a diophantine-like condition:  $|k \cdot Ak| \geq \gamma/|k|^\tau$  for any  $k \in \mathbb{Z}^2 \setminus 0$ .

$\S$  Again, to prevent diffusion on exponentially long times one should require an algebraic condition, such as:  $|k \cdot Ak| \geq \gamma/|k|^\tau$  for any  $k \in \mathbb{Z}^2 \setminus 0$ .

We say that the real function  $h : \mathcal{D} \rightarrow \mathbb{R}$ , with  $\mathcal{D} \subseteq \mathbb{R}^n$  open set, is rationally convex at  $I \in \mathcal{D}$  if its hessian matrix  $h''(I)$  is rationally convex.

We briefly explain (15) in the case  $n = 3$ . The resonances related to the lattices of dimension 1 generated by  $k \in \mathbb{Z}^3 \setminus 0$  have equations:  $k \cdot AI = 0$ . The space of fast drift is a line parallel to  $k$ , therefore a line of fast drift is contained in the resonance if and only if  $k \cdot Ak = 0$ , as in the case  $n = 2, d = 1$ . Instead, if  $n = 3, d = 2$  the resonance related to the integer vectors  $k^1, k^2$  is the line in the intersection of the planes  $k^1 \cdot AI = 0$  and  $k^2 \cdot AI = 0$ . The space of fast drift of this resonance has dimension 2, and is generated by  $k^1, k^2$ . Therefore, the resonance is transverse to the plane of fast drift if and only if equation (15) is satisfied. This argument can be generalized to the higher dimensional cases.

**Remark.** Condition (15) for any  $d = 1, \dots, n - 1$  is indeed necessary, as it can be seen considering the example  $h = (1/2)(I_1^2 - \alpha I_2^2 - \beta I_3^2)$ , with  $\alpha = 2 + \sqrt{2}$  and  $\beta = \sqrt{2}$ . Denoting  $A = h''$ , it is:  $k \cdot Ak \neq 0$  for any  $k \in \mathbb{Z}^3 \setminus 0$ . In fact, for any integer vector  $k$ , it is:  $k \cdot Ak = k_1^2 - (2 + \sqrt{2})k_2^2 - \sqrt{2}k_3^2 = (k_1^2 - 2k_2^2) - \sqrt{2}(k_2^2 + k_3^2)$  which vanishes if and only if  $k_2^2 + k_3^2 = 0$  and  $k_1^2 - 2k_2^2 = 0$ , which in turn are solved only by  $k_1 = k_2 = k_3 = 0$ . However,  $h$  is not rationally convex because it fails condition (15) for the resonance generated by  $k = (1, 0, 1)$  and  $k' = (0, 1, 1)$ . In fact, denoting by  $\tilde{K}$  the matrix whose columns are the vectors  $k, k'$ , it is :

$$\tilde{K}^T A \tilde{K} = \begin{pmatrix} k \cdot Ak & k \cdot Ak' \\ k' \cdot Ak & k' \cdot k' \end{pmatrix} = \begin{pmatrix} 1 - \beta & -\beta \\ -\beta & -\alpha - \beta \end{pmatrix} \quad (16)$$

whose determinant is  $-(1 - \beta)(\alpha + \beta) - \beta^2 = 0$ .

In the rationally convex case, it should be possible to prove exponential stability even if the proof is quite long because it reproduces the well known proof of the Nekhoroshev theorem for the convex case (see [21]). More precisely in order to prevent diffusion over times slower than exponentials of  $1/\varepsilon$  one needs some algebraic condition, such as:

$$\left| \det(\tilde{K}^T A \tilde{K}) \right| \geq \frac{\gamma}{\|\tilde{K}\|^\tau} \quad (17)$$

for any integer matrix  $\tilde{K}$  ( $\|\tilde{K}\|$  denotes a matrix-norm). In the case  $n = 2$  this condition is:

$$|Ak \cdot k| \geq \frac{\gamma}{\|k\|^\tau} \quad \forall k \in \mathbb{Z}^2 \setminus 0 \quad (18)$$

Recently, Niederman reconsidered the Morbidelli and Guzzo idea and generalized it to the generic steepness case [22].

### 3. The model problem

In this article, we study numerically the effective impact of the rational convexity on diffusion, and we compare it with the Arnold diffusion. We will use as model problem

the quasi-integrable map:

$$\begin{aligned} \varphi'_1 &= \varphi_1 + I_1 & , & \quad \varphi'_2 = \varphi_2 - \alpha I_2 \\ I'_1 &= I_1 + \varepsilon \frac{\partial f}{\partial \varphi_1}(\varphi'_1, \varphi'_2) & , & \quad I'_2 = I_2 + \varepsilon \frac{\partial f}{\partial \varphi_2}(\varphi'_1, \varphi'_2) \end{aligned} \quad (19)$$

which is in the form (5), with  $n = 2$ ,  $h$  equal to (13) and we use as perturbation the function:

$$f = \frac{1}{\cos(\varphi_1) + \cos(\varphi_2) + 2 + c} \quad , \quad c > 0 \quad .$$

This peculiar form of the perturbation is chosen because it has a full Fourier spectrum. We study the diffusion properties of the system for (many) different values of the parameter  $\alpha$ , that determines if the integrable approximation is convex ( $\alpha < 0$ ) or not ( $\alpha > 0$ ). In the non convex case we will consider separately the cases:  $\sqrt{\alpha} \in \mathbb{R} \setminus \mathbb{Q}$  (rationally convex) and  $\sqrt{\alpha} \in \mathbb{Q}$ .

In order to adapt to symplectic maps the discussion done about the hamiltonian case we recall that the geometry of resonances of a map of the form (5) is equivalent to the geometry of resonances of the hamiltonian with  $n + 1$  degrees of freedom (see [16],[17],[18])

$$h(I_1, \dots, I_n) + 2\pi I_{n+1}$$

which, in the specific case of the map (19), projects in the space of the actions  $I_1, \dots, I_n$  on the web of lines:

$$k_1 I_1 - \alpha k_2 I_2 + 2\pi k_3 = 0$$

with  $k_1, k_2, k_3 \in \mathbb{Z}$ . Then, when  $\varepsilon \neq 0$ , one can construct the normal form adapted to a resonance, such that the action dynamics is flattened near the line of fast drift that is parallel to the vector  $(k_1, k_2)$  (see [18]).

As a result, the map (19) has a generic geometry of resonances. In fact, the resonances of the unperturbed system related to all integer vectors  $(k_1, k_2, k_3)$  constitute a dense web in action plane  $(I_1, I_2)$ , while the Arnold web is a dense set in phase space. Repeating the argument given for the hamiltonian case, and recalling that the line of fast drift is parallel to  $(k_1, k_2)$ , the map (19) can have fast diffusion only if  $\alpha$  satisfies condition (14). In this case, there exists a family of resonances that potentially support fast diffusion, precisely all resonances related to integer vectors  $(k_1, k_2, k_3)$  with  $(k_1, k_2)$  satisfying:

$$\frac{k_1}{k_2} = \pm \frac{n_1}{n_2} = \pm \sqrt{\alpha} \quad ,$$

and therefore all resonant lines with equation:

$$\alpha I_2 = \pm \sqrt{\alpha} I_1 + 2\pi \frac{k_3}{k_2} \quad . \quad (20)$$

This family of resonances constitutes a web, that we call “fast web”, and is a subset of the Arnold web.

Because the fast web is dense in the action plane, the phenomenon of fast diffusion can bring the orbits near any point of phase space. In fact, diffusing orbits can in



principle change several resonances in short times of order  $1/\varepsilon$ . As a consequence, the orbits can indeed diffuse in the fast web, rather than simply drifting along a line like the simpler  $n = 2$  hamiltonian case. This justifies the use of the name 'fast diffusion' for this phenomenon.

Although the steepness hypothesis is no more valid, it still exists a part of the Arnold web that can support action diffusion with a speed that is at most exponentially slow, as in the usual Arnold diffusion. This part is the complement of the "fast web".

The size of the harmonics related to a given resonance is another relevant factor in determining the rate of diffusion. It is related to the order  $|k| = |k_1| + |k_2|$ . We remark that the fast web contains resonances with minimum order  $n_1 + n_2$ , that gives a lower bound to the speed of fast diffusion determined by  $n_1, n_2$ .

Therefore the diffusion on the resonances of the fast web of sufficiently high order can be slower than the Arnold diffusion. The typical situation, in the non rational convex case is therefore the presence of two competing mechanisms of diffusion, which is analyzed in section 4.

In the rational convex case, fast diffusion cannot exist. Indeed we find numerically that the diffusion coefficient decreases with  $\varepsilon$  faster than any power law (possibly exponentially). Nevertheless, we find that the diffusion coefficient decreases slower than the convex case. We expect such a behaviour: when matrix  $A$  satisfies a condition like (18) (which is the case that we will consider) the constant  $b$  that characterizes the stability times in (3) is smaller for large  $\tau$ . The convex case corresponds to the smallest possible value  $\tau = -2$ , i.e. to the biggest constant  $b$  in (3).

From a technical point of view, we investigate the diffusion properties of the map (19) with the techniques used in [23], [24], [25], [26], [27]. These techniques rely essentially on the so-called Fast Lyapunov Indicator (FLI in the following, introduced in [28]), that allows a precise numerical detection of the Arnold web of a given system. The theoretical motivations for the use of the FLI are reviewed in the Appendix.

#### 4. Geometry of resonances and diffusion

The numerical study of the diffusion properties of a quasi-integrable system is greatly simplified by the computation of its geometry of resonances. In fact, different kinds of diffusion can be detected in a quasi-integrable system, such as the widely observed Chirikov diffusion ([29]), the Arnold diffusion (occurring on much longer times and therefore only recently numerically detected [25], [26]) and the fast diffusion.

All these diffusion mechanisms are strictly related to the geometry of resonances: the first one is characterized by resonance overlapping, while in the second and third case resonances are arranged as a regular web (the so-called Arnold web) and the phase space is filled by a large number of invariant tori.

A precise numerical detection of the Arnold web is possible with the Fast Lyapunov Indicator (hereafter called FLI). This method, introduced by Froeschlé et al. [28] is reviewed in the Appendix. Figure 1 shows the Arnold web for the mapping (19) with

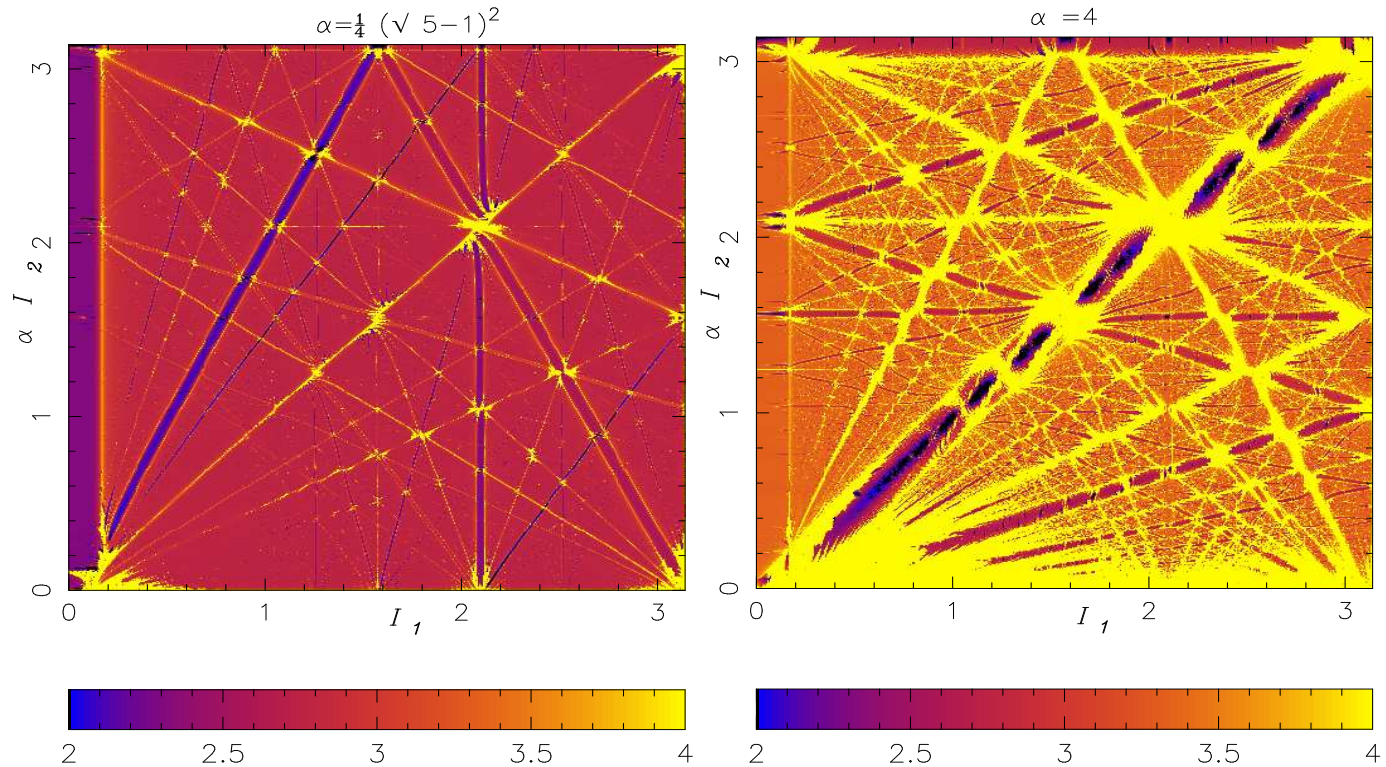


**Figure 1.** Detection of the Arnold web for a rationally convex case:  $\alpha = (\sqrt{5} - 1)^2/4$  and for  $\alpha = 4$ . The perturbation parameter is  $\varepsilon = 0.1$  and the integration time is  $t = 1000$  iterations. The FLI values close to  $\log t = 3$  correspond to invariant tori, higher values show the presence of chaotic orbits and lower values correspond to the regular part of resonances.

$\varepsilon = 0.1$ . The FLI has been computed on a set of  $500 \times 500$  initial conditions regularly spaced in the intervals:  $0 < I_1 < \pi$  and  $0 < \alpha I_2 < \pi$  for  $\alpha = (\sqrt{5} - 1)^2/4$  (Fig.1,left) and for  $\alpha = 4$  (Fig.1,right). The initial angles are chosen equal to zero and the integration time is  $t = 1000$  iterations.

In Fig.1 the white lines (yellow in the electronic version) correspond to the chaotic part of the resonances while the grey (red) background corresponds to the set of invariant tori characterized by a FLI value of about  $\log t = 3$ . Colors going from grey (red) to black stay for regular resonant motions. The Arnold web, which is a neighbourhood of all straight lines:

$$k_1 I_1 - \alpha k_2 I_2 + 2\pi k_3 = 0$$

with  $k_1, k_2, k_3 \in \mathbb{Z}$ , appears clearly. The set of all resonances is dense on the plane. However, one can expect that resonant orbits surround each resonance line up to a distance which decreases with the order  $|k| = \sum |k_i|$ . Both pictures represent a system with no global overlapping of resonances, although for  $\alpha = 4$  larger chaotic regions appear.

We recall that for  $\alpha$  satisfying condition (14) there is a family of resonances potentially supporting fast diffusion. More precisely there are the resonances related

to integer vectors  $(k_1, k_2, k_3)$  with  $(k_1, k_2)$  satisfying:

$$\frac{k_1}{k_2} = \pm \frac{n_1}{n_2} = \pm \sqrt{\alpha} \quad ,$$

and therefore all resonant lines with equation:

$$\alpha I_2 = \pm \sqrt{\alpha} I_1 + 2\pi \frac{k_3}{k_2} \quad . \quad (21)$$

This family of resonances constitutes the “fast web”. Some of these lines appear clearly on Fig.1,right.

In order to have the chance to observe fast diffusion, it is useful to select chaotic initial conditions on the fast web. This task is made easy by the FLI chart of resonances. Following the same procedure used in [25] we integrate such chaotic orbits and we represent them on the FLI chart considering only those points of the orbits which intersect the section

$$S = \{(I_1, I_2) \in \mathbb{R}^2, \varphi_i = 0, i = 1, 2\} \quad . \quad (22)$$

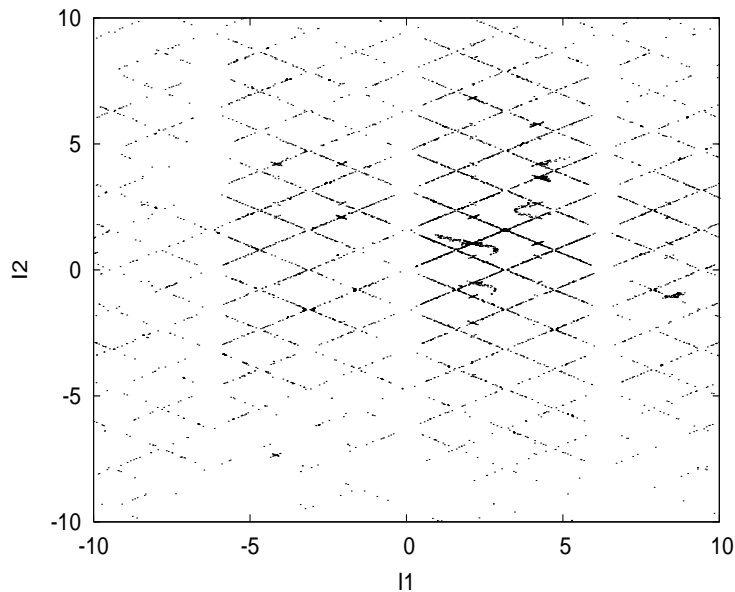
We recall that the FLI charts are obtained for initial conditions that belong to the section  $S$ . Since computed orbits are discrete, we represented points on the double section  $|\varphi_1| \leq 0.05, |\varphi_2| \leq 0.05$ . A smaller tolerance (lower than 0.05) reduces only the number of points on the section, but does not change their diffusion properties. Fig.2 shows the successive intersections of a set of 100 orbits with section  $S$  up to a time  $t = 5 \cdot 10^8$  for  $\alpha = 4$  and  $\varepsilon = 0.1$ . The initial conditions have been chosen along  $I_2 = I_1/2$  with  $0 < I_1 < \pi$ . We have checked, on a small integration time of  $t = 1000$  iterations that such orbits are chaotic, i.e. they have FLI values 20% greater than the reference value for the tori (which is  $\simeq \log t$ ). The initial angles are equal to zero.

Fig.2 shows a phenomenon of diffusion, involving a macroscopic region of the phase space. Such global diffusion occurs mainly on the “fast web”. We remark that the initial conditions were chosen on the fast web and a question may arise as to what happens when choosing initial conditions along another resonance.

We recall that in [26] we performed a similar experiment with convex systems (hamiltonian and maps) that satisfy the hypotheses of the Nekhoroshev theorem. Indeed, by selecting chaotic initial conditions on low order resonances, we have observed a phenomenon of global diffusion through all the resonances (at least of low order) of the Arnold web on times longer than any power law, and compatible with the exponential (3).

The Arnold diffusion is present also in the non-convex case, and could also play an important role. For the non convex case with  $\alpha = 4$ , we have selected a set of 100 chaotic initial conditions on the resonance  $I_2 = I_1/\alpha$  (that is not in the fast web) and represented their orbits on the FLI chart. Let us remark that the order of this resonance is  $|k| = 2$ , while the order of the resonances of the fast web satisfies  $|k| \geq n_1 + n_2 = 3$ .

We have observed that for  $\varepsilon = 0.1$  the Arnold diffusion on a time of about  $5 \cdot 10^7$  iterations moves some of the orbits through the Arnold web giving them the possibility



**Figure 2.** Diffusion for  $\varepsilon = 0.1$  of a set of 100 chaotic orbits for  $\alpha = 4$ . The points are the intersections of the orbits with the section  $S$  up to a time  $t < 5 \cdot 10^8$  iterations. It appears clearly that diffusion occurs mainly on the “fast” web, i.e. the web formed by the set of lines:  $I_2 = \pm \frac{1}{\sqrt{\alpha}} I_1 + \frac{2\pi k}{\alpha}$ , with  $k \in \mathbb{Z}$ .

of reaching the “fast web” and then rapidly diffusing. Qualitatively we observe the same pattern of Fig.2 up to  $t = 5 \cdot 10^8$  iterations.

In next sections we will study in more detail the interplay between Arnold diffusion and fast diffusion. The strategy will consist of integrating orbits that have a great probability of diffusing in both cases, i.e. chosen respectively on the low order resonance  $I_2 = I_1/\alpha$  and on the fast web.

For this purpose let us consider the rationally convex case of Fig.1, left corresponding to  $\alpha_{rc} = (\sqrt{5} - 1)^2/4$ . In this non-convex case, the lines of fast drift do not correspond to resonances. The diffusion along the resonances is of Arnold type and needs very long times to be observed according to the value of  $\varepsilon$  and to the order of the considered resonances. We have chosen a set of 100 initial conditions on the low order resonance  $I_2 = I_1/\alpha$  in the interval  $0.7 < I_1 < 0.8$ . For comparison with the convex case we have integrated 100 chaotic orbits, chosen on the same resonance, but for  $\alpha_c = -\alpha_{rc}$ . Fig.3 shows the successive intersections of the set of orbits with section  $S$  up to  $t = 10^6$  (left panel) and  $t = 10^9$  (right panel) for respectively  $\alpha_{rc}$  (top) and  $\alpha_c$  (bottom) for  $\varepsilon = 0.21$ . In both cases, we observe a local phenomenon of Arnold diffusion along the resonant line and qualitatively the only difference is the speed of diffusion, which is lower in the convex case as we remarked in Section 3.



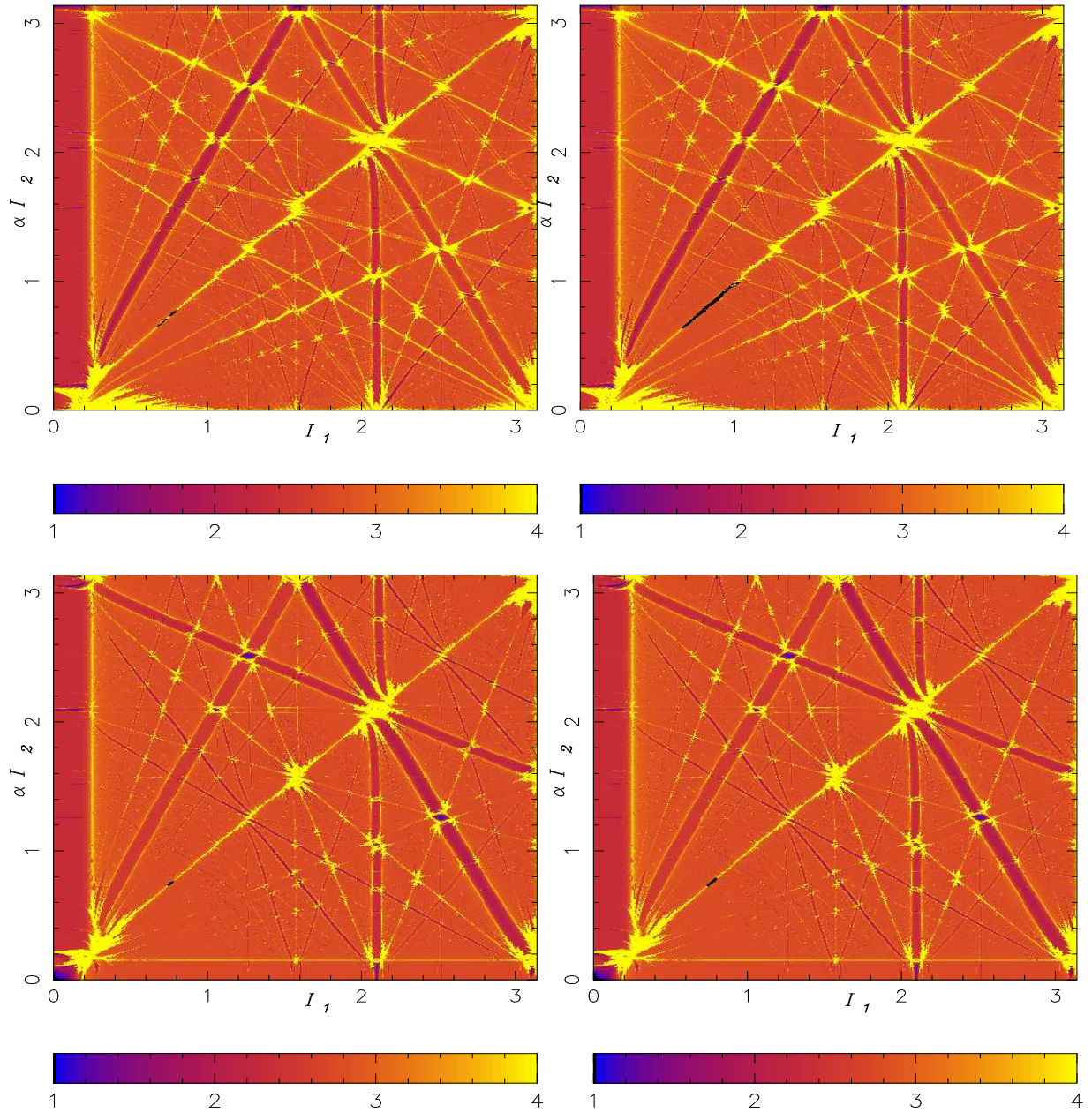


**Figure 3.** Diffusion along the resonant line  $\alpha I_2 = I_1$  for  $\varepsilon = 0.21$  of a set of 100 initial conditions with  $I_1$  in the interval  $0.7 < I_1 < 0.8$  for respectively  $\alpha_{rc} = ((\sqrt{5} - 1)/2)^2$  (top) and  $\alpha_c = -\alpha_{rc}$  (bottom). The black points are the intersections of the orbits with the section  $S$  (defined in the text) up to time  $t = 10^6$  (left panels) and  $t = 10^9$  (right panels).

## 5. Measure of the diffusion coefficient

Following the procedure of [25] we tried to measure a diffusion coefficient as if the phenomenon was Brownian like. For a chosen fraction  $T$  of the integration time, for any  $n \in \mathbb{N}$ , denoting with  $I_{1,j}(0)$  and  $I_{2,j}(0)$ ,  $j = 1, \dots, N$  the initial conditions of a set of  $N$  orbits and with  $I_{1,j}(t)$  and  $I_{2,j}(t)$  the corresponding values at time  $t$  we considered the quantity:

$$d(nT) = \frac{1}{M_n} \sum_{j: (|\varphi_{1,j}(t)| \leq 0.05, |\varphi_{2,j}(t)| \leq 0.05)} [(I_{1,j}(t) - I_{1,j}(0))^2 + (I_{2,j}(t) - I_{2,j}(0))^2] \quad (23)$$

where  $M_n$  is the number of points on section  $S$  for  $t$  in the interval  $(n-1)T \leq t \leq nT$ . In our numerical experiences we have observed a linear increase with time of  $d$ . The slope of the regression line is the diffusion coefficient  $D$ .

We have studied the dependence of the diffusion coefficient on the parameter  $\varepsilon$  for the rationally convex case with  $\alpha_{rc} = ((\sqrt{5}-1)/2)^2$  and, for comparison, for the convex case with  $\alpha_c = -((\sqrt{5}-1)/2)^2$ .

According to the experience shown in Fig.3 we have integrated, up to  $t = 10^9$  iterations, a set of 100 chaotic orbits with initial conditions chosen on the low order resonance  $I_2 = I_1/\alpha$  and we have repeated the computation for different values of  $\varepsilon$ .

The estimates of  $D$  versus  $1/\varepsilon$  are reported in Fig.4 in a logarithmic scale. Clearly, data are not well fitted with a linear regression, which would correspond to a power law  $D(\varepsilon) = C(1/\varepsilon)^m$ . Indeed, if we define 3 different sets of data, and we perform local regressions for each set, we find for  $\alpha_c$ , the three different slopes  $n_1 = -1.9$ ,  $n_2 = -5$  and  $n_3 = -15$ . This is sufficient to exclude a global power law and the changes of slope are compatible with the expected exponential decrease of  $D$ . For the non convex case with  $\alpha_{rc}$ , we have also found three different slopes  $m_1 = -3$ ,  $m_2 = -4.8$  and  $m_3 = -9$ . Such changes of slopes are in favor of an exponential decrease of  $D$  although, in agreement with the theory, slower than in the convex case.

For the non-convex and non rational convex value  $\alpha_{nc} = 4$  we have repeated the experience considering two sets of initial conditions: set (A) on the resonance  $I_2 = \frac{1}{\sqrt{\alpha}}I_1$  (that is in the fast web) and set (B) on the resonance  $I_2 = \frac{1}{\alpha}I_1$  (that is not in the fast web). Results on diffusion are presented in Fig.5. For the three larger values of  $\varepsilon$  we have observed Chirikov diffusion. Its speed is independent on the set (A) or (B) of initial conditions. For lower values of  $\varepsilon$ , when we have no resonance overlapping, we still observe a global diffusion but of different nature. Such a diffusion occurs mainly along the resonances of the “fast web” as explained in the previous Section (Fig.2).

We have observed the global diffusion on the “fast web” for all the values of  $\varepsilon$  considered for set (A) and the diffusion coefficient is well fitted by a power law (with slope  $m = -1.3$ ).

For set (B) we observe the same kind of global fast diffusion only for  $3 < 1/\varepsilon < 10$ . We can fit the points corresponding to global diffusion (both Chirikov and fast) with a power law of slope  $m_1 = -3.7$  (Fig.5). For lower values of  $\varepsilon$  only local Arnold diffusion along the resonance  $I_2 = \frac{1}{\alpha}I_1$  is observed up to  $t = 5 \cdot 10^8$  iterations. The corresponding

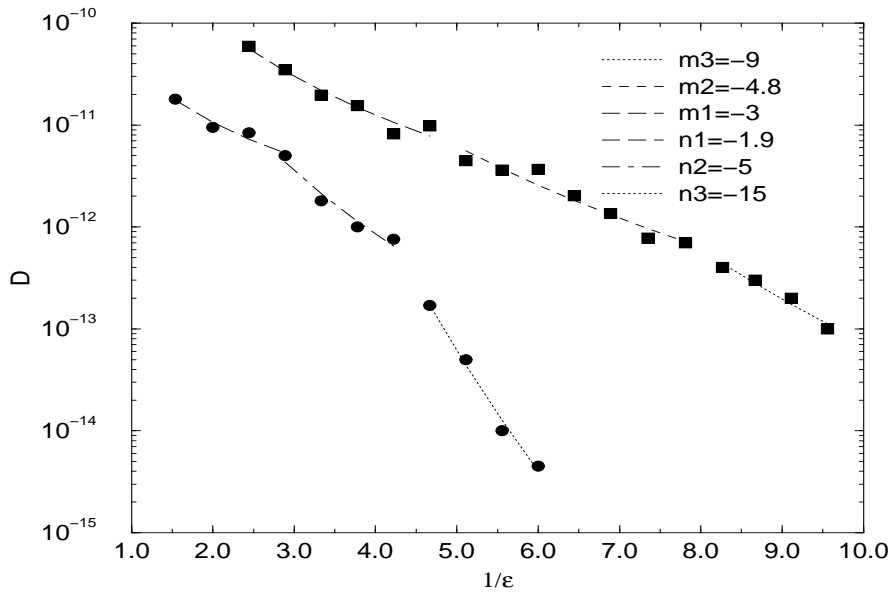


**Figure 4.** Measure of the diffusion coefficient as a function of  $1/\varepsilon$  for respectively the rationally convex case with  $\alpha_{rc}$  (square) and the convex case with  $\alpha_c = -\alpha_{rc}$ . In both cases data are well fitted by 3 power laws with slopes  $m_i$ ,  $i = 1, ..3$  for  $\alpha_{rc}$  and  $n_i$ ,  $i = 1, ..3$  for  $\alpha_c$ .

diffusion coefficient suddenly drops being fitted by a power law of slope ( $m_2 = -11$ ). For values of  $\varepsilon$  lower than 0.03 we did not observe any more diffusion up to  $t = 5 \cdot 10^8$ . Let us remark that the change of slope of set (B) is not of the same kind than the one presented in Fig.4. Here, it corresponds to the change from global (Chirikov and fast) diffusion to the local Arnold diffusion while in the previous experiment we had always the same phenomenon of local diffusion.

## 6. About the influence of $\alpha$ on the speed of diffusion.

In order to study the influence of  $1/\sqrt{\alpha}$  on the speed of diffusion in the non convex case we have measured the diffusion coefficient  $D$  for 300 values of  $\alpha$  with  $0.5 < 1/\sqrt{\alpha} < 1$ . For each value of  $\alpha$  a set of 100 chaotic initial conditions has been selected along the resonance  $I_2 = I_1/\sqrt{\alpha}$  with  $0 < I_1 < \pi$  and the orbits are computed on  $10^8$  iterations. The perturbing parameter is  $\varepsilon = 0.1$ .

Fig.6 shows the variation of the logarithm of  $D$  as a function of  $1/\sqrt{\alpha}$ . We observe a drop of 4 orders of magnitude in  $D$  when passing from  $1/\sqrt{\alpha} = 0.5$  to  $1/\sqrt{\alpha} \simeq 0.55$ . The same occurs when going from  $1/\sqrt{\alpha} = 1$  to  $1/\sqrt{\alpha} \simeq 0.9$ . Surprisingly, we do not remark the effect of the low order rational  $1/\sqrt{\alpha} = 2/3$ . The values of the diffusion coefficient around  $2/3$  are quasi constant around the value  $D \simeq 10^{-10}$ .

We have explored with more detail the case  $\alpha = 9/4$ . We considered a set of 100

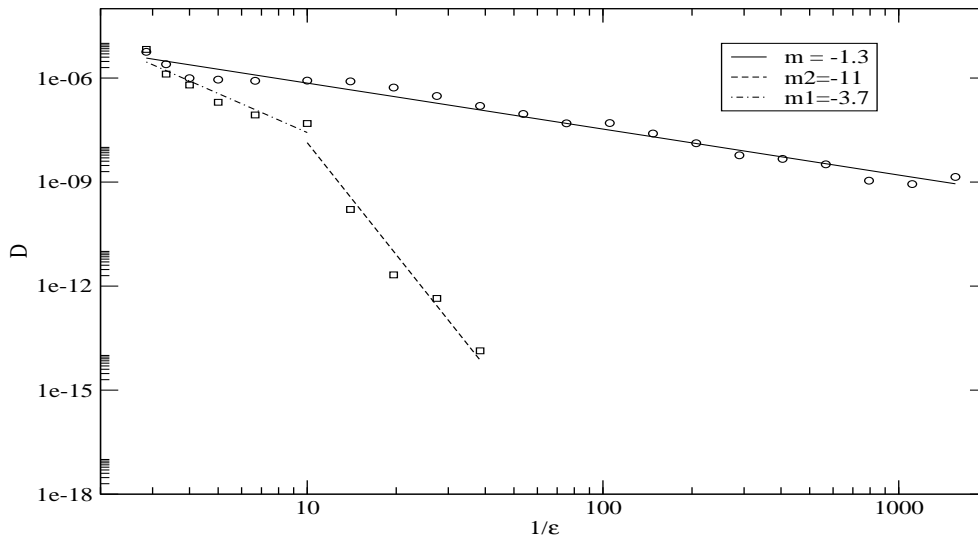


**Figure 5.** Measure of the diffusion coefficient  $D$  as a function of  $1/\varepsilon$  for orbits of data set (A) (circle) and of data set (B) (square). For data set (A) the function  $D(\varepsilon) = (1/\varepsilon)^m$  with  $m = -1.3$ . For data set (B) the diffusion coefficient is fitted by a power law with  $m_1 = -3.7$  up to  $\varepsilon = 10$  (global diffusion), then a change of slope is observed with  $m_2 = -11$  (local Arnold diffusion).

initial conditions along a resonance of fast diffusion  $I_2 = 2/3I_1$  with  $1 < I_1 < 1.3$  (data set 1) and a set of 100 initial conditions along a resonance of low order:  $I_2 = I_1/\alpha$  with  $1 < I_1 < 1.3$  (data set 2) for different values of  $\varepsilon$  (from  $\varepsilon = 0.22$  to  $\varepsilon = 0.0001$ ). The initial angles are  $\varphi_1 = 0$  and  $\varphi_2 = 0$ .

Fig.7,top shows the resulting diffusion for respectively data set 1 (left) and 2 (right) for  $\varepsilon = 0.18$ , and Fig.7,bottom for  $\varepsilon = 0.025$ . It appears clearly that, for  $\varepsilon = 0.18$  we have a phenomenon of global diffusion for both data sets, and that the speed of diffusion seems to be of the same order. More precisely, we observe that the speed of Arnold diffusion on a low order resonance can be of the same order of magnitude, or even greater than the speed of the diffusion along the fast drift line when such a line coincides with an higher order resonance. Let's recall that the order of the fast drift resonance is  $|k| = 5$  while the resonance  $I_2 = I_1/\alpha$  has order  $|k| = 2$ . Such a result is a little surprising since we are used to think to Arnold diffusion as a very slow phenomenon. Actually, when  $\varepsilon$  approaches  $\varepsilon_0$  (3), as it is for  $\varepsilon = 0.18$ , and when the fast drift line is of moderately high order (Fig.7,top), it turns out to be competitive with the fast diffusion.

When decreasing  $\varepsilon$  the speed of Arnold diffusion on orbits of data set 2 decreases faster than the speed of diffusion of orbits of data set 1. We remark that for  $\varepsilon = 0.025$ , on a time  $t = 10^8$  iterations, the main contribution to the diffusion for data set 2 is that in the directions parallel to the fast drift lines. A measure of the diffusion coefficient



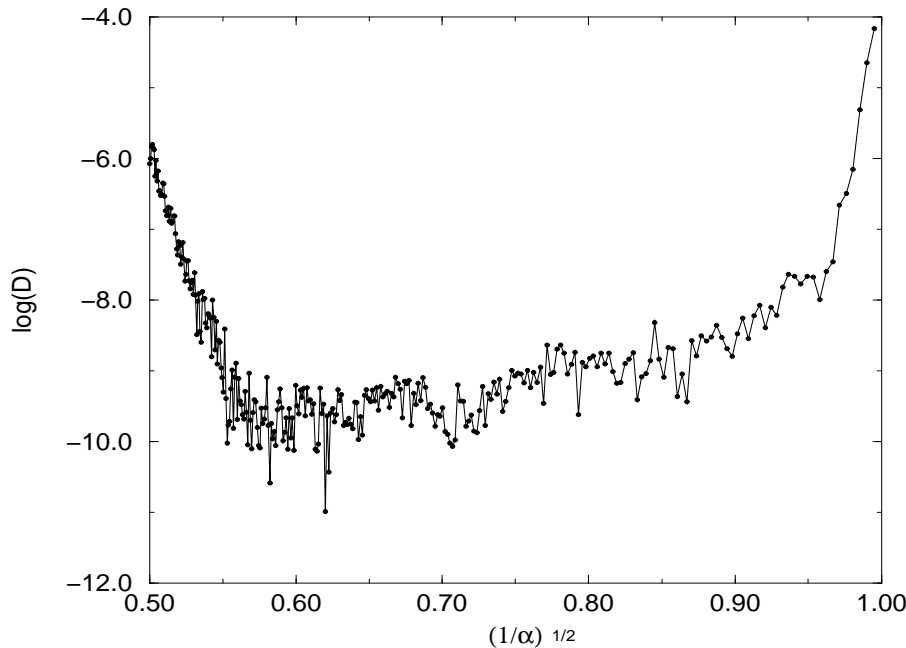


**Figure 6.** Variation of  $\log D$  as a function of  $1/\sqrt{\alpha}$  for 300 values of  $\alpha$  with  $0.5 < 1/\sqrt{\alpha} < 1$ . For each value of  $\alpha$  a set of 100 chaotic initial conditions taken along the fast drift line  $I_2 = I_1/\sqrt{\alpha}$  with  $0 < I_1 < \pi$  has been integrated up to  $t = 10^8$  iterations. The perturbing parameter is  $\varepsilon = 0.1$

(Fig.8) as a function of  $\varepsilon$  for data set 1 and 2 allows to quantify the effect of fast and of Arnold diffusion .

In particular, it appears clearly that for  $\varepsilon = 0.1$  the speed of Arnold diffusion is of the same order than the speed of fast diffusion. This is the reason why we didn't find any difference between the diffusion coefficient computed for  $1/\sqrt{\alpha} = 2/3$  and for their irrational neighbouring values. In order to observe the influence of the rational value  $1/\sqrt{\alpha} = 2/3$  on diffusion it is necessary to decrease  $\varepsilon$ . We have therefore repeated the computation of  $D$  as a function of  $1/\sqrt{\alpha}$  for 100 values in a neighbourhood of  $1/\sqrt{\alpha} = 2/3$  for  $\varepsilon = 0.05$ . Fig.9 shows the emergence of the rational value of  $1/\sqrt{\alpha} = 2/3$  characterized by a diffusion coefficient 2.5 order of magnitude higher than for  $1/\sqrt{\alpha} \simeq 2/3 \pm 0.03$ .

## 7. Conclusion

We have studied the phenomenon of diffusion in a non convex symplectic map for different values of the parameter  $\alpha$  and of the perturbation parameter  $\varepsilon$ . For  $\alpha^2 \in \mathbb{Q}$  we observed a rapid global diffusion along the resonances forming the “fast web” only when the order of the fast drift line is low. Otherwise, even if  $\alpha^2 \in \mathbb{Q}$  the diffusion along the fast drift line may not be the most rapid phenomenon. The order of the resonance

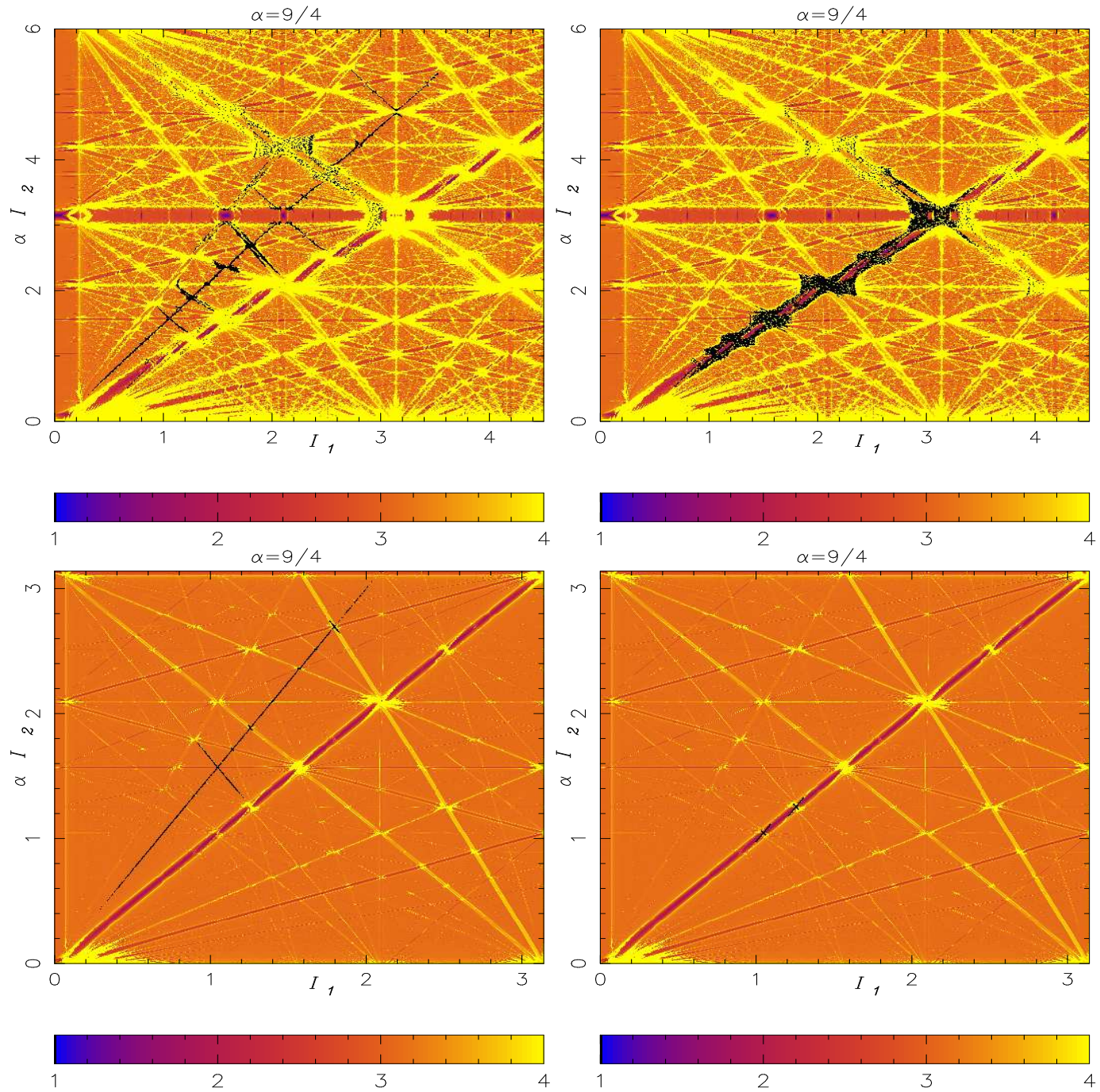


**Figure 7.** The four panels correspond to the FLI chart of the action plane  $(I_1, I_2)$  for the map, with initial conditions on the section  $S$  as explained in the text, with different magnifications. The white (yellow in the electronic version) region corresponds to the chaotic part of the Arnold web. Panel a,b are for  $\varepsilon = 0.18$  while c,d are for  $\varepsilon = 0.025$ . The black points are the intersection of the orbits with section  $S$  for data set 1 (left) and 2 (right).

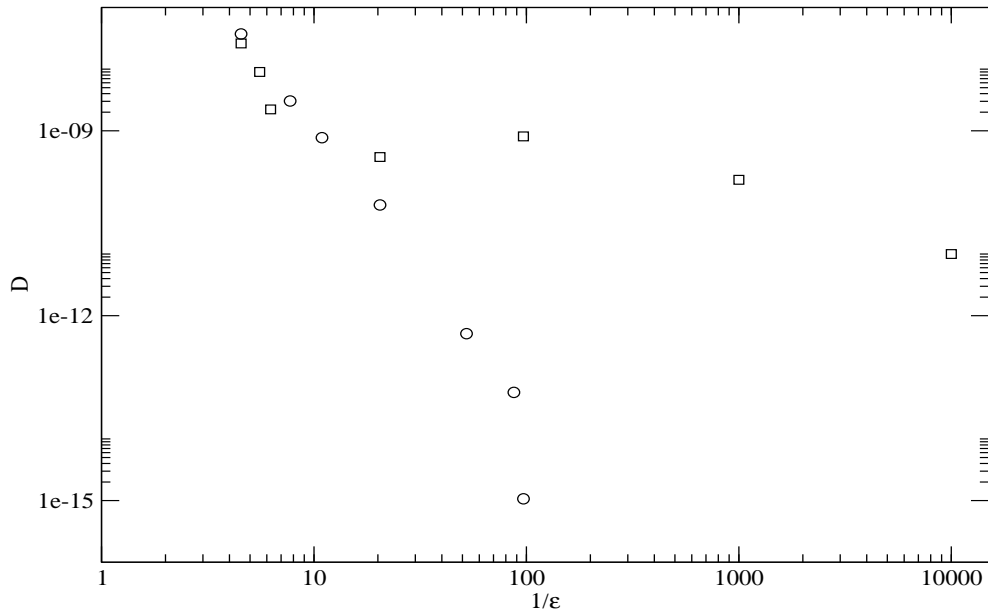


**Figure 8.**  $\alpha = 9/4$ . Variation of the diffusion coefficient as a function of  $1/\varepsilon$  for a set of 100 orbits initially chosen along the fast drift direction (square) and for a set of 100 orbits with initial conditions chosen along the low order resonance  $I_2 = I_1/\alpha$  (circles).

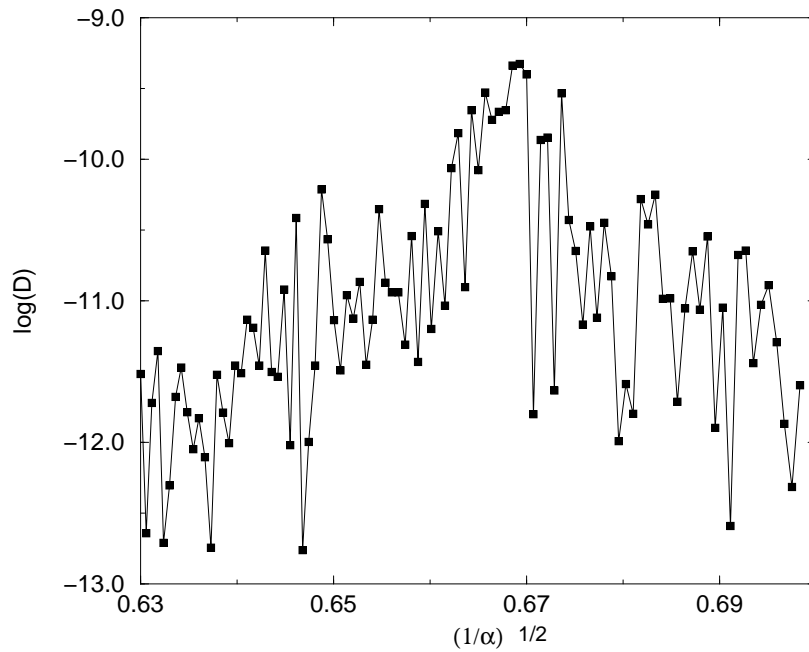


**Figure 9.** Variation of  $\log D$  as a function of  $1/\sqrt{\alpha}$  for 100 values of  $\alpha$  with  $0.63 < 1/\sqrt{\alpha} < 0.7$ . For each value of  $\alpha$  a set of 100 chaotic initial conditions taken along the fast drift line  $I_2 = I_1/\sqrt{\alpha}$  with  $0 < I_1 < \pi$  has been integrated up to  $t = 10^8$  iterations. The perturbing parameter is  $\varepsilon = 0.05$

associated to the fast drift line has to be taken into account. To be definite, we found, for some values of the perturbation parameter, a similar diffusion coefficient for orbits driven by the Arnold mechanism along a low order resonance and for orbits moving along a fast drift line coinciding with an higher order resonance. However, whatever the order of the fast drift resonance, when decreasing  $\varepsilon$  the speed of diffusion decreases slower on the fast drift direction than on other lines.

Finally, when  $\sqrt{\alpha} \in \mathbb{R}/\mathbb{Q}$  we recovered the diffusion properties of the convex case, i.e. we measured a diffusion coefficient decreasing with  $1/\varepsilon$  faster than a power law and in agreement with the expected exponential decay.

## Appendix: The FLI method and quasi-integrable dynamics

We review the FLI method showing why it allows the detection of the geometry of resonances of a quasi-integrable system. For simplicity we refer to the hamiltonian case:

$$H_\varepsilon(I, \varphi) = h(I) + \varepsilon f(I, \varphi) \quad , \quad (.1)$$

where  $I_1, \dots, I_n \in \mathbb{R}$  and  $\varphi_1, \dots, \varphi_n \in \mathbb{S}$  are action-angle variables and  $\varepsilon$  is a small parameter. For any initial condition  $(I(0), \varphi(0))$  and any initial tangent vector  $(v_I(0), v_\varphi(0))$  the Fast Lyapunov Indicator at time  $t$  is the quantity:

$$\log \|(v_I(t), v_\varphi(t))\| \quad ,$$

where  $(v_I(t), v_\varphi(t))$  is the solution of the variational equations of (.1):

$$\begin{aligned} \frac{dv_{I_j}}{dt} &= -\varepsilon \sum_{i=1}^n \frac{\partial^2 f}{\partial \varphi_j \partial I_i} v_{I_i} - \varepsilon \sum_{i=1}^n \frac{\partial^2 f}{\partial \varphi_i \partial \varphi_j} v_{\varphi_i} \\ \frac{dv_{\varphi_j}}{dt} &= \sum_{i=1}^n \frac{\partial^2 h}{\partial I_i \partial I_j} v_{I_i} + \varepsilon \sum_{i=1}^n \frac{\partial^2 f}{\partial I_i \partial I_j} v_{I_i} + \varepsilon \sum_{i=1}^n \frac{\partial^2 f}{\partial I_j \partial \varphi_i} v_{\varphi_i} \quad . \end{aligned} \quad (.2)$$

In the integrable case  $\varepsilon = 0$  the above equations are immediately integrated and the solution is

$$v_I^0(t) = v_I(0) \quad , \quad v_\varphi^0(t) = v_\varphi(0) + \frac{\partial^2 h}{\partial^2 I}(I(0))v_I(0)t \quad .$$

Therefore, the norm of the tangent vector  $v^0(t)$  grows at most linearly with time. Instead, for any  $\varepsilon \neq 0$  the system becomes non-integrable and one does not have an explicit analytic expression for the solutions of both the Hamiltonian and variational equations. However, if  $\varepsilon$  is small, one can use Hamiltonian perturbation theory to estimate the evolution of the tangent vector. Assuming that Hamiltonian (.1) satisfies the hypotheses of the KAM and Nekhoroshev theorems (in particular we assume that  $h$  is convex and  $\varepsilon$  is suitably small) we proved that [24]:

- (i) The initial condition is on a KAM torus; then the norm  $\|v^\varepsilon(t)\|$  of the tangent vector  $v^\varepsilon(t)$  integrated for the Hamiltonian  $H_\varepsilon$  satisfies:

$$\|v^\varepsilon(t)\| = \left\| \frac{\partial^2 h}{\partial^2 I}(I(0))v_I(0) \right\| t + \mathcal{O}(\varepsilon^\alpha t) + \mathcal{O}(1) \quad , \quad (3)$$

with some  $\alpha > 0$ . The reason is that the dynamics on a KAM torus corresponds to the dynamics given by an integrable Hamiltonian which is  $\varepsilon$ -close to the Hamiltonian  $h$ .

- (ii) The initial condition is on a regular resonant motion. We recall that a  $d$ -dimensional lattice  $\Lambda \subseteq Z^n$  defines a resonance through the relation:  $k \cdot \frac{\partial h}{\partial I} = 0$  for any  $k \in \Lambda$ , or equivalently:  $\Pi_\Lambda \frac{\partial h}{\partial I} = 0$  where  $\Pi_\Lambda$  denotes the Euclidean projection of a vector onto the linear space spanned by  $\Lambda$ . As is usual in the Nekhoroshev theorem, we only consider resonances related to integer lattices  $\Lambda \subseteq Z^n$  which are generated by  $d \leq n - 1$  independent integer vectors  $k^{(i)}$ ,  $i \leq d$ , with order  $|k^{(i)}| = \sum_{j=1}^n |k_j^{(i)}|$  up to a threshold order  $K$  which grows as  $1/\varepsilon^{\frac{1}{2n}}$ . According to the definitions given in [15], the resonant domain associated to a lattice  $\Lambda$  is a neighborhood of the resonance defined in the following way: first we require that the action is suitably close to the resonance through the inequality:

$$\left\| \Pi_\Lambda \frac{\partial h}{\partial I}(I(0)) \right\| \leq \frac{a_0}{(a_1 K)^{n-d} |\Lambda|} \quad (4)$$

( $a_0, a_1$  are suitable constants,  $|\Lambda|$  is the Euclidean volume of the lattice  $\Lambda$ ), second we require that  $I(0)$  is suitably far from the other resonances; more precisely we require:

$$\left\| \Pi_{\Lambda'} \frac{\partial h}{\partial I}(I(0)) \right\| > \frac{a_0}{(a_1 K)^{n-d-1} |\Lambda'|} \quad (5)$$

for any lattice  $\Lambda'$  generated by  $d + 1$  independent integer vectors of order smaller than  $K$  (we refer to the paper [15] for details). Among resonant motions it is typical to find both regular and chaotic ones. In particular, the presence of regular motions is typical in the resonances related to lattices  $\Lambda$  of dimension  $d = 1$ , because the normal form in that case depends only on one angle, and in resonances of higher multiplicity  $d > 1$  they can be found near elliptic equilibrium points, whose presence is also typical. It is also not very restrictive to assume that in the neighborhood of these elliptic equilibrium points the system satisfies the hypotheses of the KAM theorem, so that we can expect that the same neighborhood is filled with a large volume of quasi-periodic motions.

For these motions, if  $I_*, \varphi_*$  denotes the equilibrium point and one chooses an initial condition  $(I, \varphi)$  in the resonance with  $|I - I_*| \leq \sqrt{\varepsilon} \varrho$  and  $|\varphi - \varphi_*| \leq \varrho$ , then for any initial vector  $v_I(0), v_\varphi(0)$  it is [24]:

$$\|v^\varepsilon(t)\| = \|C_\Lambda \Pi_{\Lambda^{ort}} v_I(0)\| t + \mathcal{O}(\varepsilon^\beta t) + t \mathcal{O}(\varrho^2) + \mathcal{O}(\sqrt{\varepsilon} t) + \mathcal{O}\left(\frac{1}{\sqrt{\varepsilon}}\right) \quad (6)$$

with some  $\beta > 0$ ,  $\Lambda^{ort}$  being the linear space orthogonal to  $\Lambda$ , and  $C_\Lambda$  a linear operator depending on the resonant lattice  $\Lambda$  and on the initial action  $I(0)$ . It is:

$$C_\Lambda = \frac{\partial^2 h}{\partial I^2}(I(0)) - \frac{\partial^2 h}{\partial I^2}(I(0)) \left( \Pi_\Lambda \frac{\partial^2 h}{\partial I^2}(I(0)) \Pi_\Lambda \right)^* \Pi_\Lambda \frac{\partial^2 h}{\partial I^2}(I(0)) \quad , \quad (.7)$$

where  $\left( \Pi_\Lambda \frac{\partial^2 h}{\partial I^2}(I(0)) \Pi_\Lambda \right)^*$  denotes the inverse of the restriction of  $\frac{\partial^2 h}{\partial I^2}$  to the linear space spanned by  $\Lambda$  (which is well defined for the convexity of  $h$ ).

As a consequence of (.3) and (.6), the resonance structure of the phase space can be detected computing the FLI, with the same given  $v(0)$  and the same time interval  $t$  on a set of regularly spaced orbits: Eq. (.3) says that it takes approximately the value of the unperturbed case on all KAM tori; Eq. (.6) says that for suitably small  $\varepsilon$  and  $\varrho$  it is different at order  $\mathcal{O}(1)$  from the unperturbed case on regular resonant motions. In fact, the linear operator  $C_\Lambda \Pi_{\Lambda^{ort}}$  is different from the Hessian matrix of  $h$  at order  $\mathcal{O}(1)$ , i.e.  $C_\Lambda \Pi_{\Lambda^{ort}}$  does not approach  $\frac{\partial^2 h}{\partial I^2}$  as  $\varepsilon$  approaches to zero. For initial conditions on chaotic resonant motions the FLI is higher than the value characterizing KAM tori. In this way, we detect the presence of the resonances because the value of the FLI is different from the uniform value assumed on the KAM tori.

## References

- [1] A.N. Kolmogorov (1954): "On the preservation of conditionally periodic motions." Dokl. Akad. Nauk SSSR, 98, 527.
- [2] V.I. Arnol'd (1963): "Proof of A. N. Kolmogorov's theorem on the conservation of conditionally periodic motions with a small variation in the Hamiltonian." Russian Math. Surv., 18, No. 5, 9-36.
- [3] V.I. Arnol'd (1963): "Small denominators and problems of stability of motion in classical and celestial mechanics." Russ. Math. Surveys, 18, 85-191.
- [4] J. Moser (1962): On invariant curves of area preserving mappings of an annulus. Nachr. Akad. Wiss. Gött. Math. Phys. Kl., 1-20.
- [5] N.N. Nekhoroshev (1977): Exponential estimates of the stability time of near-integrable Hamiltonian systems. Russ. Math. Surveys, 32:1-65.
- [6] M. Guzzo and A. Morbidelli (1997): Construction of a Nekhoroshev like result for the asteroid belt dynamical system. Cel. Mech. and Dyn. Astron., 66:255-292.
- [7] A. Morbidelli and M. Guzzo (1997): The Nekhoroshev theorem and the asteroid belt dynamical system. Cel. Mech. and Dynam. Astron., 65:107-136.
- [8] A. Giorgilli and C. Skokos (1997): On the stability of the Trojan asteroids. Astronomy and Astrophysics, 17: 254-261.
- [9] G. Benettin, F. Fassò and M. Guzzo (1998): Nekhoroshev-stability of L4 and L5 in the spatial restricted three-body problem. Regular and chaotic dynamics, Volume 3, n. 3.
- [10] M. Guzzo, Z. Knezevic and A. Milani (2002): Probing the Nekhoroshev Stability of Asteroids. Celest. Mech. Dyn. Astr., Volume 83, Issues 1-4.
- [11] M. Guzzo (2005): The web of three-planets resonances in the outer Solar System. Icarus, vol. 174, n. 1., pag. 273-284.
- [12] N.N. Nekhoroshev (1979): Exponential estimates of the stability time of near-integrable Hamiltonian systems, 2 Trudy Sem. Petrovs., vol. 5, 5-50.
- [13] L. Niederman (2004): Exponential stability for small perturbations of steep integrable Hamiltonian systems. Ergodic Theory Dynam. Systems 24, no. 2, 593-608.

- [14] P. Lochak (1992): “Canonical perturbation theory via simultaneous approximation”. *Russ. Math. Surv.*, vol. 47, 57–133.
- [15] J. Poschel (1993): Nekhoroshev’s estimates for quasi-convex Hamiltonian systems. *Math. Z.*, 213:187–216.
- [16] S.B. Kuksin (1993): On the inclusion of an almost integrable analytic symplectomorphism into a Hamiltonian flow. *Russian journal of Mathematical Physics*, 1, 2, 191–207.
- [17] S.B. Kuksin and J. Pöschel (1994): On the inclusion of analytic symplectic maps in analytic Hamiltonian flows and its applications. *Seminar on Dynamical Systems (St. Petersburg, 1991)*, 96–116, *Progr. Nonlinear Differential Equations Appl.*, 12, Birkhäuser, Basel.
- [18] M. Guzzo (2004):” A direct proof of the Nekhoroshev theorem for nearly integrable symplectic maps”. *Annales Henry Poincaré*, vol. 5, n. 6, 1013-1039.
- [19] M. Guzzo (1999): “Nekhoroshev stability of quasi-integrable degenerate Hamiltonian systems”. *Regular and chaotic dynamics, Volume 4*, n. 2.
- [20] G. Benettin, F. Fassò and M. Guzzo (2004): Long-term stability of proper rotations of the Euler perturbed rigid body. *Commun. Math. Phys.* 250, 133-160.
- [21] G. Benettin, L. Galgani, and A. Giorgilli (1985): “A proof of Nekhoroshev’s theorem for the stability times in nearly integrable Hamiltonian systems”. *Cel. Mech.*, vol. 37, pag. 1.
- [22] L. Niederman (2004):”Prevalence of exponential stability among nearly-integrable systems”. Preprint.
- [23] C. Froeschlé, M. Guzzo, and E. Lega (2000): Graphical evolution of the Arnold web: from order to chaos. *Science*, 289 N.5487:2108–2110.
- [24] M. Guzzo, E. Lega and C. Froeschlé (2002): On the numerical detection of the stability of chaotic motions in quasi-integrable systems. *Physica D*, 163:1–25.
- [25] E. Lega, M. Guzzo, and C. Froeschlé (2003) Detection of Arnold diffusion in Hamiltonian systems. *Physica D*, 182:179–187.
- [26] M. Guzzo, E. Lega, and C. Froeschlé (2005) First numerical evidence of global Arnold diffusion in quasi-integrable systems. *DCDS-B*, 5:687–698.
- [27] C. Froeschlé, M. Guzzo, and E. Lega (2005): Local and global diffusion along resonant lines in discrete quasi-integrable dynamical systems. *Cel. Mech and Dynam. Astron.*, in press.
- [28] C. Froeschlé, E. Lega, and R. Gonczi (1997) Fast Lyapunov indicators. Application to asteroidal motion. *Celest. Mech. and Dynam. Astron.*, 67:41–62.
- [29] B. V. Chirikov (1979): An universal instability of many dimensional oscillator system. *Phys. Reports*, 52:265.